

1 **Biallelic *MFSD2A* variants associated with congenital microcephaly, developmental**
2 **delay, and recognizable neuroimaging features.**

3

4 **Running title: *MFSD2A*-related congenital microcephaly.**

5

6 The work was supported by National Research Foundation grants (NRF2016NRF-
7 NRFI001-15); Biomedical Research Council of A*STAR; March of Dimes Research
8 Grant; National Institute for Health Research University College London Hospitals
9 Biomedical Research Centre.

10

11 Marcello Scala^{1,2,3*}, Geok Lin Chua^{4*}, Cheen Fei Chin⁴, Hessa S Alsaif⁵, Borovikov
12 Artem⁶, Saima Riazuddin⁷, Sheikh Riazuddin^{8,9}, M. Chiara Manzini¹⁰, Mariasavina
13 Severino¹¹, Alvin Kuk⁴, Hao Fan^{12,13,14}, Yalda Jamshidi¹⁵, Mehran Beiraghi Toosi¹⁶,
14 Mohammad Doosti¹⁶, Ehsan Ghayoor Karimiani¹⁶, Vincenzo Salpietro^{1,2}, Elena Dadali⁶,
15 Galina Baydakova⁶, Fedor Konovalov^{17,18}, Ekaterina Lozier^{17,18}, Emer O'Connor¹, Yasser
16 Sabr¹⁹, Abdullah Alfaifi²⁰, Farah Ashrafzadeh²¹, Pasquale Striano^{2,3}, Federico Zara^{2,22},
17 Fowzan S Alkuraya^{23,24}, Henry Houlden¹, Reza Maroofian^{15¶}, David L. Silver^{4¶}.

18

19 ¹ Department of Neuromuscular Disorders, Institute of Neurology, University College
20 London, London, United Kingdom

21 ² Department of Neurosciences, Rehabilitation, Ophthalmology, Genetics, Maternal and
22 Child Health, University of Genoa, Genoa, Italy

23 ³ Pediatric Neurology and Muscular Diseases Unit, IRCCS Istituto Giannina Gaslini, Genoa,
24 Italy

25 ⁴ Signature Research Program in Cardiovascular and Metabolic Disorders, Duke-NUS
26 Medical School, Singapore, 169857, Singapore

27 ⁵ Department of Genetics, King Faisal Specialist Hospital and Research Centre, Riyadh,
28 Saudi Arabia

29 ⁶ Research Centre for Medical Genetics, Moscow, Russia

30 ⁷ Department of Otorhinolaryngology Head & Neck Surgery, School of Medicine,
31 University of Maryland, Baltimore, MD 21201, USA

32 ⁸ Center for Genetic Diseases, Shaheed Zulfiqar Ali Bhutto Medical University, Pakistan
33 Institute of Medical Sciences, Islamabad, Pakistan

34 ⁹ National Centre of Excellence in Molecular Biology, University of the Punjab, Lahore
35 53700, Pakistan

36 ¹⁰ Department of Neuroscience and Cell Biology and Child Health Institute of New Jersey,
37 Rutgers Robert Wood Johnson Medical School, New Brunswick, NJ 08901, USA

38 ¹¹ Neuroradiology Unit, IRCCS Istituto Giannina Gaslini, Genoa, Italy

39 ¹² Bioinformatics Institute, Agency for Science, Technology and Research (A*STAR), 30
40 Biopolis St., Matrix No. 07-01, Singapore, 138671, Singapore

41 ¹³ Department of Biological Sciences, National University of Singapore, 14 Science Drive
42 4, Singapore, 117543, Singapore.

43 ¹⁴ Centre for Computational Biology, DUKE-NUS Medical School, 8 College Road,

44 Singapore, 169857, Singapore

45 ¹⁵ Genetics Research Centre, Molecular and Clinical Sciences Institute, St George's,

46 University of London, Cranmer Terrace, London SW17 0RE, UK

47 ¹⁶ Department of pediatric diseases, Faculty of medicine, Mashhad University of Medical

48 Sciences, Mashhad, Iran

49 ¹⁷ Independent Clinical Bioinformatics Laboratory, Moscow, Russia

50 ¹⁸ Genomed Ltd., Moscow, Russia

51 ¹⁹ Department of Obstetrics and Gynecology, King Saudi University, Riyadh, Saudi Arabia

52 ²⁰ Pediatrics Department, Security Forces Hospital, Riyadh, Saudi Arabia

53 ²¹ Department of Pediatric Diseases, Mashhad University of Medical Sciences, Mashhad,

54 Iran

55 ²² Unit of Medical Genetics, IRCCS Istituto Giannina Gaslini, Genova Italy

56 ²³ Department of Genetics, King Faisal Specialist Hospital and Research Center, Saudi

57 Arabia

58 ²⁴ Department of Anatomy and Cell Biology, College of Medicine, Alfaisal University,

59 Riyadh, Saudi Arabia

60 * These authors contributed equally to this work

61 ¶ Correspondence should be addressed to R.M. (rmarroofian@gmail.com, +44 (0) 203448

62 [4069 \(Internal x84069\)](tel:+442034484069)) and D.L.S. (david.silver@duke-nus.edu.sg, +65 6516 7666).

63

64 **Abstract**

65 Major Facilitator Superfamily Domain containing 2a (*MFSD2A*) is an essential endothelial
66 lipid transporter at the blood-brain barrier. Biallelic variants affecting function in *MFSD2A*
67 cause autosomal recessive primary microcephaly 15 (MCPH15, OMIM# 616486). We
68 sought to expand our knowledge of the phenotypic spectrum of MCPH15 and demonstrate
69 the underlying mechanism of inactivation of the *MFSD2A* transporter. We carried out
70 detailed analysis of the clinical and neuroradiological features of a series of 27 MCPH15
71 cases, including eight new individuals from seven unrelated families. Genetic investigation
72 was performed through exome sequencing (ES). Structural insights on the human *Mfsd2a*
73 model and in-vitro biochemical assays were used to investigate the functional impact of the
74 identified variants. All patients had primary microcephaly and severe developmental delay.
75 Brain MRI showed variable degrees of white matter reduction, ventricular enlargement,
76 callosal hypodysgenesis, and pontine and vermian hypoplasia. ES led to the identification
77 of six novel biallelic *MFSD2A* variants (NG_053084.1, NM_032793.5: c.556+1G>A,
78 c.748G>T; p.(Val250Phe), c.750_753del; p.(Cys251SerfsTer3), c.977G>A; p.(Arg326His),
79 c.1386_1435del; p.(Gln462HisfsTer17), and c.1478C>T; p.(Pro493Leu)) and two recurrent
80 variants (NM_032793.5: c.593C>T; p.(Thr198Met) and c.476C>T; p.(Thr159Met)). All
81 these variants and the previously reported NM_032793.5: c.490C>A; p.(Pro164Thr)
82 resulted in either reduced *MFSD2A* expression and/or transport activity. Our study further
83 delineates the phenotypic spectrum of MCPH15, refining its clinical and neuroradiological
84 characterization and supporting that *MFSD2A* deficiency causes early prenatal brain

85 developmental disruption. We also show that poor MFSD2A expression despite normal
86 transporter activity is a relevant pathomechanism in MCPH15.

87

88 **Keywords: *MFSD2A*; microcephaly; developmental delay; brain MRI.**

89

90 **Introduction**

91 Major Facilitator Superfamily Domain containing 2a (*MFSD2A*) is a sodium-dependent
92 lysophosphatidylcholine (LPC) transporter that is highly expressed at the endothelium of
93 the blood-brain barrier (BBB).¹ Omega-3 fatty acids and other mono- and polyunsaturated
94 fatty acids conjugated as LPCs are transported by *MFSD2A*, which plays a pivotal role in
95 the supply of omega-3 fatty acids to the brain¹. The essential role of *MFSD2A* in regulating
96 lipogenesis in the developing brain has been recently demonstrated using loss-of-function
97 mouse models.²

98 Five distinct homozygous loss-of-function *MFSD2A* variants have been reported in
99 patients with neurodevelopmental abnormalities from seven consanguineous families.
100 These patients showed developmental delay (DD), microcephaly, and neuroimaging
101 abnormalities such as ventriculomegaly and hypoplasia of the corpus callosum, brainstem,
102 and cerebellum. These observations underscored the fundamental role of LPC transport at
103 the BBB for human brain development and clarified the structure-function relationships in
104 the *MFSD2A*-mediated transport mechanism.³⁻⁹

105 In this study, we report seven new families with biallelic variants affecting function
106 in *MFSD2A* , expanding the phenotype and defining the characteristic neuroimaging
107 features of *MFSD2A*-related neurodevelopmental disorder, also known as Autosomal
108 Recessive Microcephaly 15, (MCPH15, OMIM #616486). We provide clinical, genetic,
109 and functional characterization of these novel variants and the previously reported
110 NM_032793.5:c.593C>T; p.(Thr198Met) and c.490C>A; p.(Pro164Thr) variants on the
111 transporter activity, which further substantiates the functional importance of LPC transport
112 for human brain development.

113

114 **Materials and methods**

115 **Patients ascertainment**

116 Eight patients from seven unrelated families were locally referred for exome sequencing
117 (ES) in the context of severe microcephaly and psychomotor delay. Patients were enrolled
118 in accordance with the Declaration of Helsinki and informed consent was obtained for all of
119 them in agreement with the requirements of Iranian, Pakistani, Russian, and Saudi bioethics
120 laws. Subjects were examined by several geneticists, neurologists, and pediatricians with
121 expertise in pediatric neurology. Detailed family history was collected for all families.
122 Brain MRI were locally acquired with different protocols, but all included diffusion
123 weighted images, T1 and T2-weighted, and FLAIR images on the 3 planes. Images were
124 reviewed by an experienced pediatric neuroradiologist (MS) and a pediatrician with

125 expertise in neurogenetics (MS) in consensus. Blood samples were obtained from patients
126 and parents.

127

128 **Exome Sequencing**

129 After standard DNA extraction from peripheral blood, proband exome sequencing (ES) was
130 performed in all the families as previously described.¹⁰⁻¹² Variants were filtered out
131 according to frequency, conservation, and predicted impact on protein function by several
132 bioinformatic tools (SIFT, Polyphen-2, Mutation Taster). Candidate variants were
133 subsequently validated through co-segregation studies by Sanger sequencing and submitted
134 to the gene variant database LOVD at <https://databases.lovd.nl/shared/genes/MFSD2A>
135 (Individual IDs 00276067, 00276070, 00276071, 00276074, 00276075, 00276076,
136 00276077). All the variants are reported according to the NM_032793.5 transcript.
137 GeneMatcher was used for the distributed case-matching.¹³ Further details available in the
138 Supplementary Methods.

139

140 **Functional tests summary methods**

141 Site-directed mutagenesis was used to create the Mfsd2a variants
142 NM_032793.5:c.1478C>T; p.(Pro493Leu), c.593C>T; p.(Thr198Met), c.490C>A;
143 p.(Pro164Thr), c.977G>A; p.(Arg326His), and c.748G>T; p.(Val250Phe) in a mammalian
144 expression vector, which were used to determine the effects on transporter function in
145 mammalian cells. The amino acid variants in Mfsd2a protein were modeled and visualized

146 to understand the causative mechanism of transporter dysfunction. Further details are
147 available in the Supplementary Methods.

148

149 **Results**

150 **Clinical features**

151 We present eight patients (Table 1) from seven unrelated families of varying ancestry
152 (Saudi, Iranian, Pakistani, and Russian), including six consanguineous families (Families A,
153 B, C, E, F, and G) (Fig. 1a, b).

154 Patient 1 (Family A) is a 4-year-old female born to consanguineous parents (first-
155 cousins) of Iranian ancestry. Prenatal ultrasound revealed microcephaly. At birth, her
156 occipital frontal circumference (OFC) was 28 cm (-4.6 SDS). At the age of 6 months, she
157 had head-lag, was unable to roll over, and lacked babbling. At 1 year of age, she started to
158 suffer from myoclonic seizures and failure to thrive (FTT) due to dysphagia. Physical
159 examination at 4 years showed progressive microcephaly with an OFC of 41 cm (-5.6 SDS)
160 and bilateral talipes equinovarus (TEV). She was unable to walk and neurological
161 examination revealed spastic quadriparesis and hyperreflexia. Karyotyping and metabolic
162 testing were normal.

163 Patient 2 (Family B) is 4-year-old Iranian male born to consanguineous parents.
164 Family history revealed several previous miscarriages. His older brother was healthy. At
165 birth, his OFC was 27 cm (-3.9 SDS). He was diagnosed with global DD during infancy
166 and started to suffer from generalized tonic-clonic seizures since the age of 2 years. At 4

167 years, he was unable to sit and his language was very limited. Physical examination
168 revealed bilateral TEV, progressive microcephaly with OFC of 37 cm (-8.8 SDS) and
169 spastic quadriparesis.

170 Patient 3 and 4 (Family C) belong to a consanguineous family of Pakistani descent
171 consisting of six siblings. Two males were reported to have microcephaly and died in the
172 neonatal period due to a possible infection. Two males were healthy. The proband (patient
173 3), a 17-year-old female, and her sister (patient 4), currently 27 years old, presented with
174 severe global DD and aggressive behavior during infancy. They had no seizure history.
175 Physical evaluation revealed mild muscle weakness, language limited to few words, and
176 severe microcephaly, with an OFC of 49 cm (-5.0 SDS) and 47 cm (-6.9 SDS) in patients 3
177 and 4, respectively.

178 Patient 5 (Family D) is the youngest of two siblings born to unrelated parents of
179 Russian descent. Neonatal history was unremarkable except for microcephaly. The baby
180 started to suffer from generalized tonic-clonic seizures at the age of 1 month. Global DD
181 was subsequently diagnosed at 1 year of age as he was unable to sit without support and
182 could not speak. At 5 years, the patient was unable to walk and nonverbal. He had
183 microcephaly with OFC of 46 cm (-3.6 SDS), gross and fine motor impairment, and axial
184 hypotonia. He also had dysphagia, excessive drooling, and some dysmorphic features,
185 including wide nasal bridge and prominent epicanthal folds.

186 Patient 6 (Family E) is a 1-month-old Saudi female born to consanguineous parents.
187 She was the youngest of four siblings. Her older brother had microcephaly but died during
188 infancy. The patient was diagnosed with severe microcephaly at birth, with an OFC of 28.5

189 cm (-6.2 SDS). During the neonatal period she suffered from FTT due to severe dysphagia
190 and physical examination further revealed generalized spasticity.

191 Patient 7 (Family F) is a 2-year-old male born to consanguineous parents from
192 Saudi Arabia. During the neonatal period, he suffered from FTT and received percutaneous
193 endoscopic gastrostomy (PEG) due to severe dysphagia. At 1 year of age, he started to
194 suffer from recurrent seizures treated with phenobarbital and sodium valproate.
195 Developmental milestones were severely delayed. The patient was also diagnosed with
196 gastro-esophageal reflux. Physical examination showed microcephaly, bilateral TEV,
197 generalized muscle weakness, and spasticity.

198 Patient 8 (Family G) is a 4-month-old female born to consanguineous Saudi parents.
199 Prenatal ultrasound showed microcephaly and foetal echogenic bowel. Perinatal course was
200 uneventful, but at the age of 1 week the baby was admitted to neonatal intensive care unit
201 due to relevant feeding difficulties. At 4 months, she started to suffer from seizures
202 requiring hospitalization. Physical examination showed microcephaly, generalized
203 spasticity, bilateral hip dislocation, and left TEV.

204

205 **Neuroimaging**

206 Brain MRI revealed mild to severe white matter reduction with consequent ventricular
207 dilatation in all subjects (Fig. 1c). In particular, the supratentorial white matter was
208 markedly thinned with severe ventriculomegaly in 5/8 patients. The degree of myelination
209 was appropriate for the age in all subjects. The cortical gyral pattern was mildly to severely

210 simplified in all cases, without other associated cortical malformations. The thalami were
211 small and the corpus callosum was abnormal in all patients. In particular, in 5 subjects the
212 corpus callosum was markedly thin and short, in 2 patients there was hypoplasia of the
213 anterior portion of the corpus callosum, while in the remaining patient it was globally thin.
214 Of note, the cingulate gyrus was present in all subjects. Finally, inferior vermian hypoplasia
215 was observed in all cases, while pontine hypoplasia was present in 6/8 patients.

216

217 **Genetic findings**

218 After filtering for allele frequency, conservation, and predicted functional impact, biallelic
219 *MFSD2A* variants were prioritized as candidate disease-causing variants. Eight different
220 variants were identified (Fig. 1d), including three homozygous missense variants
221 (c.1478C>T; p.(Pro493Leu) in patient 1; c.593C>T; p.(Thr198Met) in patient 3 and 4;
222 c.476C>T; p.(Thr159Met) in patient 6), a homozygous splice site variant (patient 2:
223 NG_053084.1(NM_032793.5): c.556+1G>A, NC_000001.11(NM_032793.5):
224 c.556+1G>A, LRG_199t1), two homozygous frameshift variants (c.1386_1435del;
225 p.(Gln462HisfsTer17) in patient 7; c.750_753del; p.(Cys251SerfsTer3) in patient 8), and
226 two compound heterozygous missense variants (c.[748G>T];[977G>A],
227 p.[(Val250Phe)];[(Arg326His)] in patient 5) (Table 2). Biparental segregation confirmed
228 the autosomal recessive inheritance model. In Family C (Fig. 1a), unaffected individuals
229 (II-1 and II-3) were heterozygous for the c.593C>T; p.(Thr198Met) variant in *MFSD2A*,
230 whereas the DNA of the deceased individuals (II-2 and II-6) was not available due to their

231 premature death. All the identified variants are absent in the homozygous state and
232 extremely rare in the heterozygous state in the most common population databases
233 (including our database of 10,000 exomes, gnomAD, Greater Middle East Variome - GME,
234 Iranome, and Ensembl). Missense variants were located at the amino acid residues with
235 high levels of conservation, with a Genomic Evolutionary Rate Profiling (GERP) score
236 between 5.49 to 5.94. The predicted effect on protein function was also consistent with a
237 loss-of-function mechanism, with a Combined Annotation Dependent Depletion (CADD)
238 score ranging from 24.4 to 34. The two frameshift variants are predicted to result in
239 nonsense mediated mRNA decay, likely leading to a functional knock-out. All the
240 identified variants are predicted to be damaging by several bioinformatic tools, such as
241 SIFT, Polyphen-2, and Mutation Taster. The splicing variant c.556+1G>A is predicted to
242 result in aberrant splicing through the alteration of the wildtype (WT) donor site by Human
243 Splice Finder and Variant Effect Predictor.

244

245 **Mfsd2a variants lead to loss-of-function and/or loss-of-expression**

246 Human Mfsd2a is a 530 amino acid glycosylated sodium-dependent MFS transporter
247 composed of 12 conserved transmembrane domains.⁷ To understand the consequence of the
248 c.1478C>T; p.(Pro493Leu), c.490C>A; p.(Pro164Thr), c.593C>T; p.(Thr198Met),
249 c.977G>A; p.(Arg326His), and c.748G>T; p.(Val250Phe) variants on the structure and
250 function of Mfsd2a, we utilized a published structural model of human Mfsd2a to carry out
251 bioinformatic predictions.⁷ In the c.593C>T; p.(Thr198Met) mutant model, M198 faces the

252 internal cavity of the transporter and forms more favorable hydrophobic interactions with
253 neighboring residues such as F399 from helix X, in comparison to T198 in the WT model
254 that faces the membrane exterior (Fig. 1e). In the c.1478C>T; p.(Pro493Leu) mutant model,
255 the proline-to-leucine amino acid change results in the extension of helix XII that is
256 stabilized by a hydrophobic cluster formed by sidechains of L493 and three other residues
257 Y294, L297, and F489 (Fig. 1e). In addition, multiple polar interactions observed in the
258 WT model are absent in the c.1478C>T; p.(Pro493Leu) mutant model, including the
259 hydrogen bonding interaction between Y294 and E497 as well as ionic locks between R498
260 and a negatively charged surface comprising D408, D411, and D412. These ionic locks
261 were previously suggested to be important for the transporter function.⁷ Taken together, we
262 observed enhanced hydrophobic packing in both mutant models likely leading to increased
263 structure rigidity and reduced mobility of the transporter, indirectly inactivating the
264 transport of substrate. Additionally, the c.1478C>T; p.(Pro493Leu) mutant would be
265 predicted to show a reduction in transport due to the partial loss of ionic locks.

266 We next utilized HEK293 cells, which do not endogenously express Mfsd2a, as an *in*
267 *vitro* cell system to determine if Mfsd2a variants affect protein expression, localization, and
268 transport function. Mock transfected and the sodium binding transporter inactive mutant
269 p.(Asp97Ala) (p.(D97A)) served as negative controls,^{1,7} while WT Mfsd2a served as a
270 positive control. Western blot analysis of WT Mfsd2a showed the multiple protein bands
271 similar to results previously reported for overexpression of Mfsd2a in HEK293 cells,^{3,4,6}
272 while all the five mutants c.1478C>T; p.(Pro493Leu), c.593C>T; p.(Thr198Met),
273 c.490C>A; p.(Pro164Thr), c.977G>A; p.(Arg326His), and c.748G>T; p.(Val250Phe) were

274 expressed at less than 30% of WT Mfsd2a (Fig.2a). This low level of protein expression of
275 these five Mfsd2a mutants is consistent with predicted negative effects of these variants on
276 protein folding (Fig. 1e). Despite low level expression of all five Mfsd2a mutants,
277 immunofluorescence microscopy indicated that all mutants were expressed at the plasma
278 membrane similarly to WT (Fig. 2b).

279 To directly test the functional consequences of these five variants on LPC transport,
280 we utilized an established transport assay that quantifies net transport of ^{14}C -LPC-DHA in
281 HEK293 cells. To directly compare transport activity between WT and the five mutants
282 c.1478C>T; p.(Pro493Leu), c.593C>T; p.(Thr198Met), c.490C>A; p.(Pro164Thr),
283 c.977G>A; p.(Arg326His), and c.748G>T; p.(Val250Phe), we first titrated down the
284 amount of plasmid DNA for the transfection of WT Mfsd2a into cells to obtain a
285 comparable expression level of WT to all five mutants. We found that 0.1 μg of WT
286 yielded similarly low levels of expression as cells transfected with 2 μg of mutants (Fig. 2c).
287 Surprisingly, at comparable protein expression levels of WT and mutants, four of the five
288 mutants demonstrated comparable transport of ^{14}C -LPC-DHA in HEK293 cells with
289 c.593C>T; p.(Thr198Met) at 75%, c.490C>A; p.(Pro164Thr) at 82%, c.977G>A;
290 p.(Arg326His) at 104%, and c.748G>T; p.(Val250Phe) at 80% of WT transport activity.
291 Only P493L was similar to non-functional D97A negative control, indicating it is inactive
292 (Fig. 2d).

293 Previously reported non-synonymous variants in Mfsd2a have been shown to affect
294 transport function but not protein expression.^{3,4,6} In our cases, five of the variants
295 (c.593C>T; p.(Thr198Met), c.490C>A; p.(Pro164Thr), c.977G>A; p.(Arg326His),

296 c.748G>T; p.(Val250Phe), and c.1478C>T; p.(Pro493Leu)) were extremely lowly
297 expressed (Fig. 2a). Our findings indicate that poor expression of Mfsd2a, despite normal
298 transporter activity, can also be an underlying cause for severe microcephaly and
299 hypomyelination in these patients, which further defines the etiology of Mfsd2a-related
300 microcephaly.

301

302 **Discussion**

303 MFSD2A is a sodium-dependent 12-pass transmembrane protein belonging to the major
304 facilitator superfamily of secondary transporters. Mfsd2a plays a pivotal role at the BBB for
305 the transport of plasma-derived LPCs conjugated to polyunsaturated fatty acids such as the
306 omega-3 fatty acid docosahexaenoic acid (DHA) to the brain.^{1,2,14} The deficiency of the
307 DHA in the brain of *Mfsd2a*-knockout mice is associated with a severe neurodevelopmental
308 phenotype characterized by microcephaly, cognitive impairment, ataxia, and severe
309 anxiety.¹² In particular, microcephaly is likely explained by the fact that LPC transport not
310 only provides accretion of DHA by the developing brain, but is also critical for providing
311 LPC as building blocks for neuron arborization and regulation of membrane phospholipid
312 composition.^{2,5,15} The reports of loss-of-function *MFSD2A* variants in patients with a
313 progressive microcephaly syndrome with severe ID and neuroimaging abnormalities have
314 supported the relevant role of this lipid transporter in human brain development and
315 functioning.^{3,4,9} The relevance of proper DHA metabolism for brain development and
316 functioning is further supported by CYP2U1 deficiency. This enzyme is a member of the

317 cytochrome P450 family 2 subfamily U and catalyzes the hydroxylation of arachidonic acid
318 (AA) and AA-related long-chain fatty acids, including DHA.¹⁶ Biallelic loss-of-function
319 *CYP2U1* variants cause spastic paraplegia 56 (SPG56), a complex neurological condition
320 characterized by spasticity, cognitive impairment, and white matter abnormalities.¹⁶

321 Here, we present seven families with eight distinct loss-of-function variants in
322 *MFSD2A*, including seven novel variants affecting function. Patient 4 was part of a large
323 cohort of consanguineous families with recessive intellectual disability reported by
324 Riazuddin et al.⁸ Patients 6 and 7 were briefly described before by Shaheen et al. and
325 Monies et al., respectively.^{17,18} In line with previously reported cases, our patients showed a
326 complex neurodevelopmental phenotype primarily characterized by severe progressive
327 microcephaly, ID, spasticity, and speech delay (Table 1) (Fig. 1f).^{3,4,6,8,9} Less common
328 clinical features were also identified in our cohort, including axial hypotonia, increased
329 deep tendon reflexes, and seizures (Fig. 1b).^{3,4,6,8,9} Of note, none of our patients died
330 prematurely, although some of their siblings who died prematurely were most likely
331 affected by the same condition. The longest follow-up was 27 years (patient 4), allowing
332 assessment of the progression of microcephaly over time. Language was delayed in most
333 subjects and one patient was nonverbal. Four patients showed skeletal abnormalities
334 consistent with TEV. Dysmorphic features were observed in patient 5 only.

335 In previously reported cases, brain MRI revealed a spectrum of abnormal findings,
336 including ventricular enlargement secondary to white matter paucity and hypoplasia of the
337 corpus callosum, cerebellum, and brainstem.^{3,4} In our study, we provide further evidence
338 that affected subjects present severe microcephaly with simplified gyral pattern, associated

339 with variable degrees of white matter reduction leading to mild to severe ventricular
340 dilatation. Of note, the myelination was always appropriate for patients' age in our series,
341 ruling out a hypomyelinating disorder. Interestingly, the corpus callosum was always
342 abnormal, with severe hypodysplasia in most subjects. However, the cingulate gyrus was
343 present in the most severe cases as well, indicating that the corpus callosum was initially
344 formed. Finally, the inferior cerebellar vermis was small in all subjects while hypoplasia of
345 the pons was noted in almost all of them. Taken together, these neuroimaging features are
346 consistent with an early prenatal developmental disruption and likely suggest a relevant role
347 of LPCs in the development of both the cerebral gray and white matter.

348 A clear correlation between the severity of the clinico-radiological phenotype and the
349 variants affecting function in *MFSD2A* could not be observed. Despite the *MFSD2A*
350 variants identified in the current study impair protein expression rather than the transporter
351 function, no substantial difference between the phenotypes of previously reported affected
352 individuals and patients from the current cohort was noticed (Table 1). This observation
353 supports the loss of function as the main pathogenic mechanism in MCPH15, regardless of
354 the specific underlying cause. All patients show a variable degree of progressive
355 microcephaly and a comparable level of psychomotor delay, but some speculations on
356 selected phenotypic features are possible. In fact, behavioural disturbances appeared to be
357 more frequent in subjects carrying missense variants affecting the transporter function
358 (c.1016C>T; p.(Ser339Leu), c.476C>T; p.(Thr159Met), and c.497C>T; p.(Ser166Leu)),^{3,4}
359 whereas skeletal abnormalities might be more common in patients carrying variants
360 resulting in decreased MFSD2A expression, as showed by patients 1, 2, 7, and 8 from our

361 cohort. Interestingly, extrapyramidal disorders have been associated with the previously
362 reported variants c.1205C>A; p.(Pro402His) and c.490C>A; p.(Pro164Thr),^{6,9} but were
363 absent in our cases. As to the neuroimaging features, the degree of involvement of grey and
364 white matter structures is quite variable in the affected individuals and does not appear to
365 be correlated to *MFSD2A* variant type.

366 In conclusion, our observations expand the phenotypic spectrum of *MFSD2A*-related
367 microcephaly syndrome and provide new insights into the underlying pathogenic
368 mechanisms. Refining the neuroradiological characterization of MCPH15, we suggest that
369 some neuroimaging clues can be extremely relevant for an early diagnosis. We also show
370 that poor *MFSD2A* expression plays a relevant role in MCPH15 pathogenesis, further
371 defining the etiology of this condition. A better understanding of the role of *MFSD2A* in
372 brain physiology will foster the development of targeted therapies or specific metabolic
373 supplementation regimens to bypass LPC transport deficiency. The identification and
374 characterization of further patients harboring loss-of-function *MFSD2A* variants will
375 support efforts to exploit LPCs as therapeutic lipids to improve DHA delivery and promote
376 proper brain development in affected individuals.

377

378 **Acknowledgments**

379 The work was supported in part by National Research Foundation and Ministry of Health
380 grants, Singapore; by the Biomedical Research Council of A*STAR; by March of Dimes
381 Research Grant; as part of the Queen Square Genomics group at University College

382 London, supported by the National Institute for Health Research University College
383 London Hospitals Biomedical Research Centre.

384

385 **Conflict of Interest**

386 The authors declare no conflict of interest.

387

388 **Funding**

389 National Research Foundation grants, Singapore NRF2016NRF-NRFI001-15 and OF-IRG
390 MOH-000217 (to D.L.S.); Biomedical Research Council of A*STAR (to H.F.); The MRC
391 (MR/S01165X/1, MR/S005021/1, G0601943), The National Institute for Health Research
392 University College London Hospitals Biomedical Research Centre, Rosetree Trust, Ataxia
393 UK, MSA Trust, Brain Research UK, Sparks GOSH Charity, Muscular Dystrophy UK
394 (MDUK), Muscular Dystrophy Association (MDA USA), March of Dimes USA (to
395 M.C.M.), The R01 RNS107428A by the National Institute of Neurological Disorders and
396 Stroke/National Institutes of Health (NINDS/NIH).

397 **References**

- 398 1. Nguyen LN, Ma D, Shui G, Wong P, Cazenave-Gassiot A, Zhang X, et al. Mfsd2a is a
399 transporter for the essential omega-3 fatty acid docosahexaenoic acid. *Nature*. 2014;509:503-6.
- 400 2. Chan JP, Wong BH, Chin CF, Galam DLA, Foo JC, Wong LC, et al. The lysolipid transporter
401 Mfsd2a regulates lipogenesis in the developing brain. *PLoS Biol*. 2018;16:e2006443.
- 402 3. Alakbarzade V, Hameed A, Quek DQ, Chioza BA, Baple EL, Cazenave-Gassiot A, et al. A
403 partially inactivating mutation in the sodium-dependent lysophosphatidylcholine transporter
404 MFSD2A causes a non-lethal microcephaly syndrome. *Nat Genet*. 2015;47:814-7.
- 405 4. Guemez-Gamboa A, Nguyen LN, Yang H, Zaki MS, Kara M, Ben-Omran T, et al.
406 Inactivating mutations in MFSD2A, required for omega-3 fatty acid transport in brain, cause a
407 lethal microcephaly syndrome. *Nat Genet*. 2015;47:809-13.
- 408 5. Guesnet P, Alessandri JM. Docosahexaenoic acid (DHA) and the developing central nervous
409 system (CNS) - Implications for dietary recommendations. *Biochimie*. 2011;93:7-12.
- 410 6. Harel T, Quek DQY, Wong BH, Cazenave-Gassiot A, Wenk MR, Fan H, et al. Homozygous
411 mutation in MFSD2A, encoding a lysolipid transporter for docosahexanoic acid, is associated
412 with microcephaly and hypomyelination. *Neurogenetics*. 2018;19:227-35.
- 413 7. Quek DQ, Nguyen LN, Fan H, Silver DL. Structural insights into the transport mechanism of
414 the human sodium-dependent lysophosphatidylcholine transporter Mfsd2a. *J Biol Chem*.
415 2016;291:9383-94.
- 416 8. Riazuddin S, Hussain M, Razzaq A, Iqbal Z, Shahzad M, Pollaet DL, et al. Exome sequencing
417 of Pakistani consanguineous families identifies 30 novel candidate genes for recessive
418 intellectual disability. *Mol psychiatry*. 2017;22:1604-14.
- 419 9. Hu H, Kahrizi K, Musante L, Fattahi Z, Herwig R, Hosseini M, et al. Genetics of intellectual

420 disability in consanguineous families. *Mol Psychiatry*. 2019;24:1027-39.

421 10. Li H, Durbin R. Fast and accurate short read alignment with Burrows-Wheeler transform.
422 *Bioinformatics*. 2009;25:1754-60.

423 11. Van der Auwera GA, Carneiro MO, Hartl C, Poplin R, Del Angel G, Levy-Moonshine A,
424 et al. From FastQ data to high confidence variant calls: the Genome Analysis Toolkit best
425 practices pipeline. *Curr Protoc Bioinformatics*. 2013;43:11.10.1-11.10.33.

426 12. Wang K, Li M, Hakonarson H. ANNOVAR: functional annotation of genetic variants
427 from high-throughput sequencing data. *Nucleic Acids Res*. 2010;38:e164.

428 13. Sobreira N, Schiettecatte F, Valle D, Hamosh A. GeneMatcher: a matching tool for
429 connecting investigators with an interest in the same gene. *Hum Mutat*. 2015;36:928-30.

430 14. Andreone BJ, Chow BW, Tata A, Lacoste B, Ben-Zvi A, Bullock K, et al. Blood-Brain
431 Barrier Permeability Is Regulated by Lipid Transport-Dependent Suppression of Caveolae-
432 Mediated Transcytosis. *Neuron*. 2017;94:581-94.

433 15. Ahmad A, Moriguchi T, Salem N. Decrease in neuron size in docosahexaenoic acid
434 deficient brain. *Pediatr Neurol*. 2002;26:210-8.

435 16. Tesson C, Nawara M, Salih MA, Rossignol R, Zaki MS, Al Balwi M, et al. Alteration of
436 fatty-acid-metabolizing enzymes affects mitochondrial form and function in hereditary spastic
437 paraplegia. *Am J Hum Genet*. 2012;91:1051-64.

438 17. Shaheen R, Maddirevula S, Ewida N, Alsahli S, Abdel-Salam GMH, Zaki MS, et al.
439 Genomic and phenotypic delineation of congenital microcephaly. *Genet Med*. 2019;21:545-52.

440 18. Monies D, Abouelhoda M, Assoum M, Moghrabi N, Rafiullah R, Almontashiri N, et al.
441 Lessons Learned from Large-Scale, First-Tier Clinical Exome Sequencing in a Highly
442 Consanguineous Population. *Am J Hum Genet.* 2019;104:1182-201.

443

444 **Legends**

445 **Fig. 1 Clinical characterization, neuroimaging features, genetic findings and predicted**
446 **consequences of *MFSD2A* variants.** (a) Pedigrees of the seven reported families. (b) Main
447 clinical features include severe microcephaly, axial hypotonia, talipes equinovarus, and minor
448 dysmorphic features (e.g., epicanthal folds and broad nasal bridge in patient 5). (c) Brain MRI of
449 affected subjects performed at 3 years (Pt 1), 1 year (Pt 2), 17 years (Pt 3), 27 years (Pt 4), 2
450 months (Pt 5), 1 month (Pt 6), 2 years (Pt 7), and 4 months of age (Pt 8). First row: axial T2,
451 FLAIR or T1-weighted images of the patients. Second row: corresponding sagittal T2 or T1-
452 weighted images. There is severe microcephaly with mildly to severely simplified gyral pattern
453 in all subjects. The cerebral white matter is reduced with consequent ventricular dilatation
454 (asterisks), especially in patients 1, 2, 6, 7, and 8. The corpus callosum is barely visible and
455 markedly short in patients 1, 2, 6, 7, and 8 (empty arrows), while it is diffusely hypoplastic in
456 Patient 5. Hypoplasia of the anterior portion of the corpus callosum is visible in patients 3 and 4
457 (arrows). Note that in all subjects the cingulate gyrus is present. The inferior portion of the
458 vermis is small in all subjects (arrowheads), with associated pontine hypoplasia in patients 1, 2, 5,
459 6, 7, and 8. (d) 3D structural model of *Mfsd2a* (based on Quek DQ et al., 2016; Supplementary
460 References) indicating the locations of previously reported variants (in black) and the variants
461 identified in this study (in red). The N-terminus is indicated in green and C-terminus in cyan. (e)

462 3D structural models of the Mfsd2a variants. Positions of variants in the human Mfsd2a protein.
463 Variants (cyan) were mapped to the published homology model of Mfsd2a (green). R326 is
464 located at the putative extracellular gate and the R326H substitution might disrupt gate closure.
465 V250 and P164 are both located in helical bundles. Their substitution by larger amino acids
466 (V250F and P164T) might perturb protein folding by steric clash with neighboring sidechains
467 (e.g., W134, W118). P164T might also form a hydrogen bond with Y49 that is not seen in
468 canonical Mfsd2a. Variants T198M and P493L are predicted to alter the local protein structure.
469 (f) Percentage distribution of the main clinical features of *MFSD2A* patients. *DD* developmental
470 delay; *ID* intellectual disability; *N/A* not applicable; *Pt* patient.

471

472 **Fig. 2 Biochemical analysis of Mfsd2a variants.** (a) Western blot probed for Mfsd2a and its
473 mutants with β -actin used as loading control. (b) Confocal immunofluorescence micrographs of
474 transiently transfected HEK293 cells with Mock, WT, D97A, P493L, T198M, P164T, R326H
475 and V250F variants affecting function showing Mfsd2a localization in green cell nuclei in blue
476 (Hoechst stain), red arrows pointing to the cell surface localization of Mfsd2a and its mutants. (c)
477 Titration of varying amounts of WT Mfsd2a DNA (μ g) to normalize the expression levels to
478 determine the amount of WT Mfsd2a needed for comparable expression levels with cells
479 transfected with 2 mg of mutant construct DNA. (d) Transport of 50 μ M 14 C LPC-DHA by
480 comparable expression levels of *MFSD2A* in HEK293. Significance levels of difference
481 compared with the transport activity of 0.1 μ g of WT Mfsd2a (labeled WT on the graph)
482 transport activity are labeled with asterisks; **** representing P value < 0.0001, ***
483 representing P value <0.001, ** representing P value < 0.01, * representing P value <0.1.

Table 1. Genetic, clinical, and neuroradiological features of *MFSD2A* patients.

<i>Families</i>	<i>A (Pt 1)</i>	<i>B (Pt 2)</i>	<i>C (Pt 3)</i>	<i>C (Pt 4)[#]</i>	<i>D (Pt 5)</i>	<i>E (Pt 6)^{##}</i>	<i>F (Pt 7)^{###}</i>	<i>G (Pt 8)</i>	<i>Alakbarzade, 2015 (10 pts)</i>	<i>Guemez-Gamboa, 2015 (4 pts)[†]</i>	<i>Harel, 2018 (2 pts)</i>	<i>Hu, 2019 (3 pts)</i>
<i>Age (last FU), sex</i>	4 y, F	4 y, M	17 y, F	27 y, F	5 y, M	1 mo, F	2 y, M	4 mo, F	Mean 12.6 y M/F = 2.3	Mean N/A M/F = 0.3	Mean 4.9 y M/F = 1	Mean 22 y M/F = 0.5
<i>Origin</i>	Iran	Iran	Pakistan	Pakistan	Russia	Saudi	Saudi	Saudi	Pakistan	Libya, Egypt	Jewish Moroccan	Iran
<i>Consanguinity</i>	+	+	+	+	-	+	+	+	+	+	+	+
<i>MFSD2A variant [NM_032793.5]</i>	c.[1478C>T]; [1478C>T], p.[(Pro493Leu)]; [(Pro493Leu)]	c.[556+1G>A]; [556+1G>A] [‡]	c.[593C>T]; [593C>T], p.[(Thr198Met)]; [(Thr198Met)]	c.[593C>T]; [593C>T], p.[(Thr198Met)]; [(Thr198Met)]	c.[748G>T]; [c.977G>A], p.[(Val250Phe)]; [(Arg326His)]	c.[476C>T]; [476C>T], p.[(Thr159Met)]; [(Thr159Met)]	c.[1386_1435del]; [1386_1435del], p.[(Gln462HisfsTer17)]; [(Gln462HisfsTer17)]	c.[750_753del]; [750_753del], p.[(Cys251SerfsTer3)]; [(Cys251SerfsTer3)]	c.[1016C>T]; [1016C>T], p.[(Ser339Leu)]; [(Ser339Leu)]	Fam 1825 c.[476C>T]; [476C>T], p.[(Thr159Met)]; [(Thr159Met)] Fam 1422 c.[497C>T]; [497C>T], p.[(Ser166Leu)]; [(Ser166Leu)]	c.[1205C>A]; [1205C>A], p.[(Pro402His)]; [(Pro402His)]	c.[490C>A]; [c.490C>A], p.[(Pro164Thr)]; [(Pro164Thr)]
<i>OFC at birth</i>	28 cm (-4.6 SDS)	27 cm (-3.9 SDS)	N/A	N/A	N/A	28.5 cm (-3.6 SDS)	25.5 cm (-6 SDS)	30.5 cm (-2.4 SDS)	N/A	Mean -1.3 SDS	Mean -2.5 SDS	N/A
<i>OFC at FU</i>	41 cm (-5.6 SDS)	37 cm (-8.8 SDS)	49 cm (-5.0 SDS)	47 cm (-6.9 SDS)	46 cm (-3.6 SDS)	N/A	36 cm (-8.9 SDS)	36 cm (-3.9 SDS)	</-3 SDS	Mean -5 SDS	Mean -3.25 SDS	Mean -4.3 SDS
<i>GDD</i>	+	+	+	+	+	+	+	+	+	+	+	+
<i>Sitting</i>	-	-	+	+	+	-	-	+	N/A	+	+	+
<i>Walking</i>	-	-	+	+	-	-	-	-	N/A	-	-	+
<i>Speech</i>	Non-verbal	Severely Delayed	Severely Delayed	Severely Delayed	Non-verbal	Non-verbal	Non-verbal	Non-verbal	Absent/limited (10/10)	Non-verbal (3/3)	Severely Delayed (2/2)	Non-verbal (2/3)
<i>ID</i>	N/A	N/A	Severe	Severe	Severe	Severe	Severe	Severe	Severe (10/10)	+	+	+
<i>Behavioural abnormalities</i>	-	-	Aggressive	Aggressive	-	-	-	-	ASD (10/10)	ASD (3/3)	-	-
<i>Appendicular spasticity</i>	+	+	+	+	-	+	+	+	+	+	+	-
<i>Axial hypotonia</i>	+	-	-	-	+	-	-	-	N/A	+	+	-
<i>Seizures</i>	+	+	-	-	+	+	+	+	-	+	-	-
<i>Dysphagia</i>	+	-	-	-	+	+	+	+	N/A	+	-	-
<i>Skeletal abnormalities</i>	TEV	TEV	-	-	-	-	TEV	TEV, Bilateral DDH	N/A	TEV (2/3)	-	-
<i>Premature death</i>	-	-	-	-	-	-	-	-	N/A	+	-	-
<i>MRI findings</i>												
<i>WM thinning with ventricular dilatation</i>	Severe	Severe	Moderate	Moderate	Mild	Severe	Severe	Severe	+	+	+	N/A

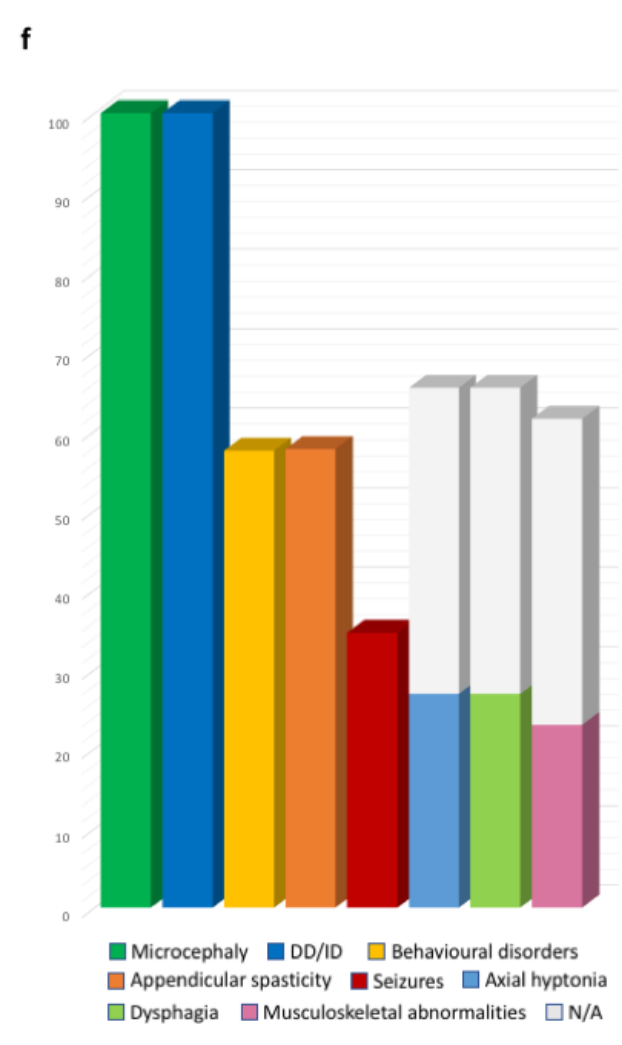
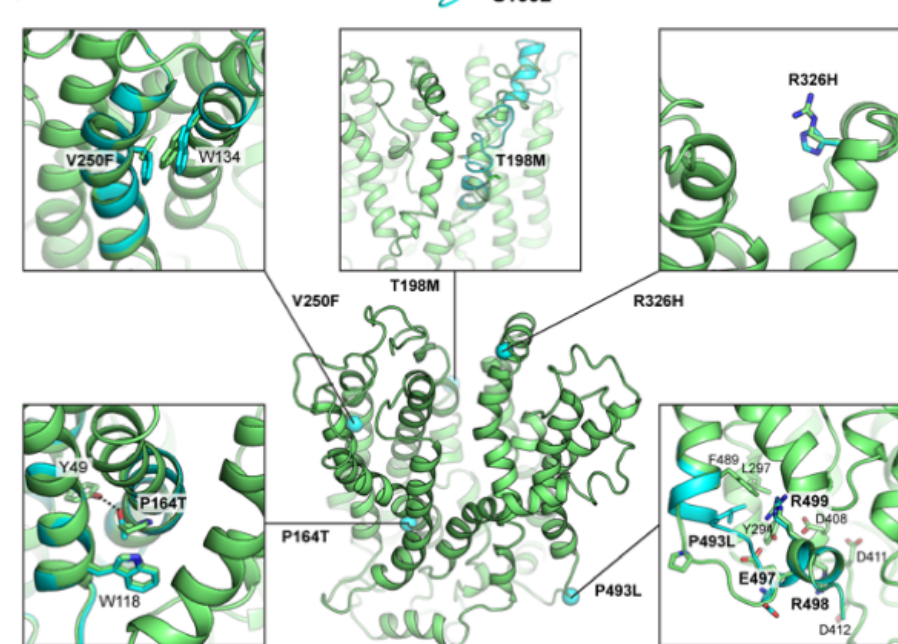
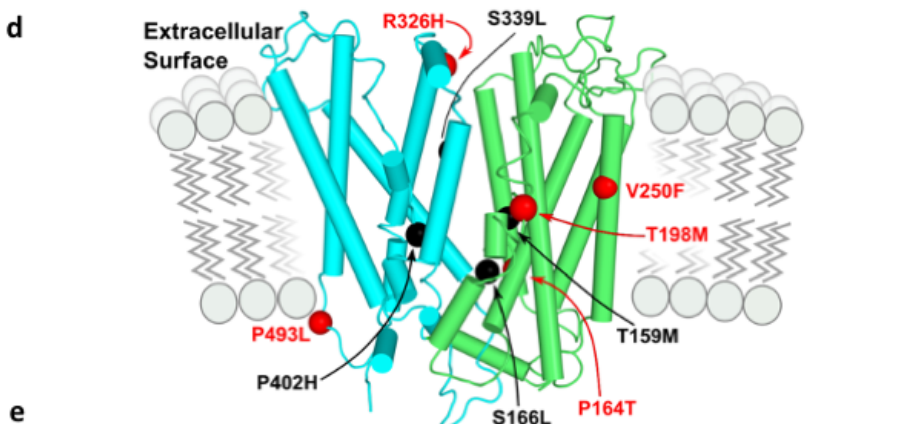
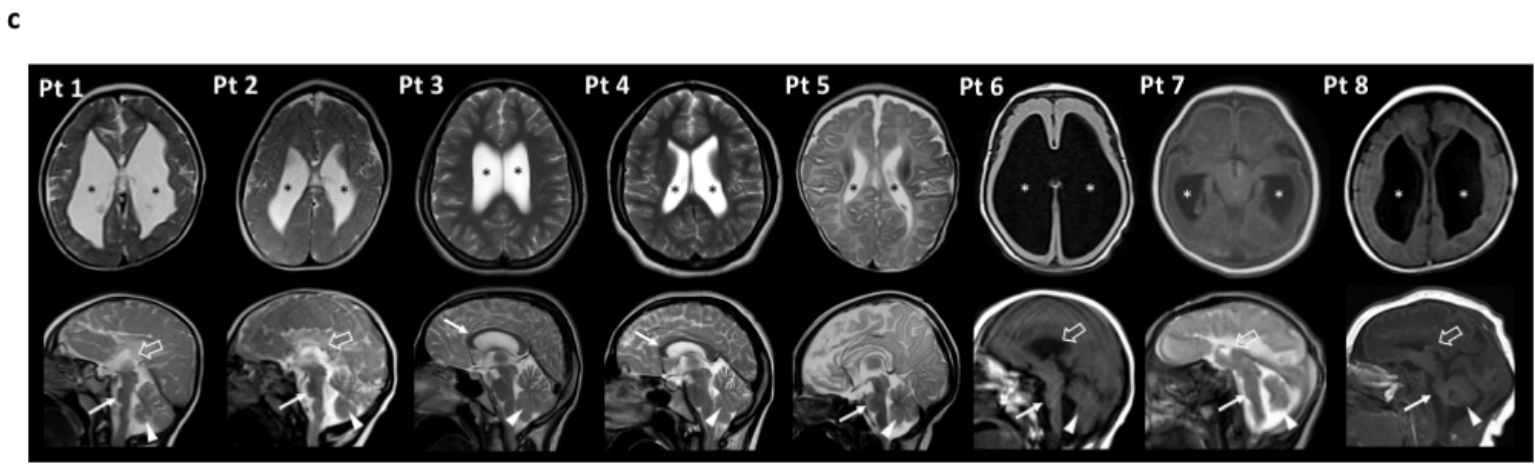
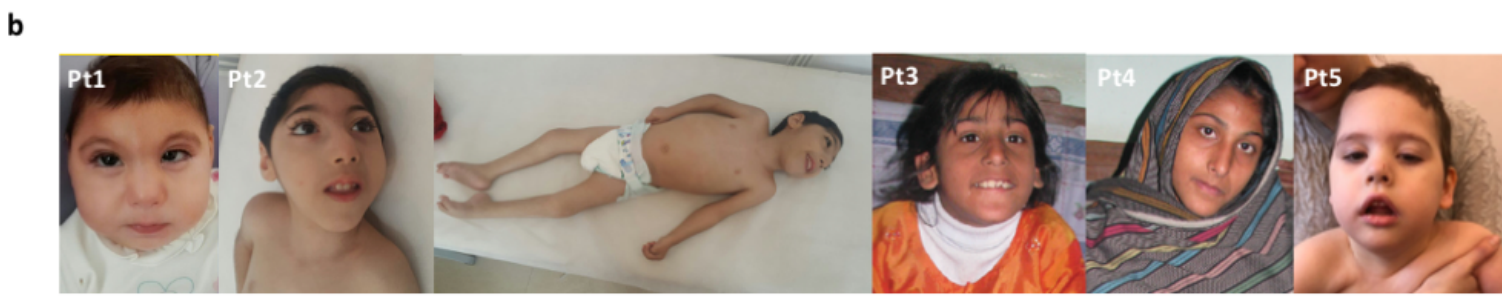
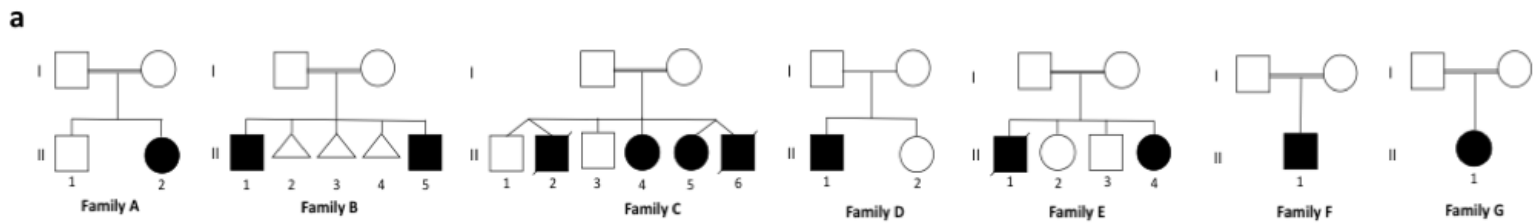
<i>Simplified gyral pattern</i>	Severe	Severe	Mild	Mild	Mild	Severe	Severe	Severe	N/A	N/A	N/A	N/A
<i>Corpus callosum hypoplasia</i>	Severe	Severe	Mild	Mild	Mild	Severe	Severe	Severe	N/A	+ (3/3)	N/A	N/A
<i>Inferior vermian hypoplasia</i>	+	+	+	+	+	+	+	+	N/A	+ (3/3)	N/A	N/A
<i>Pontine hypoplasia</i>	+	+	-	-	-	+	+	+	N/A	N/A	N/A	N/A

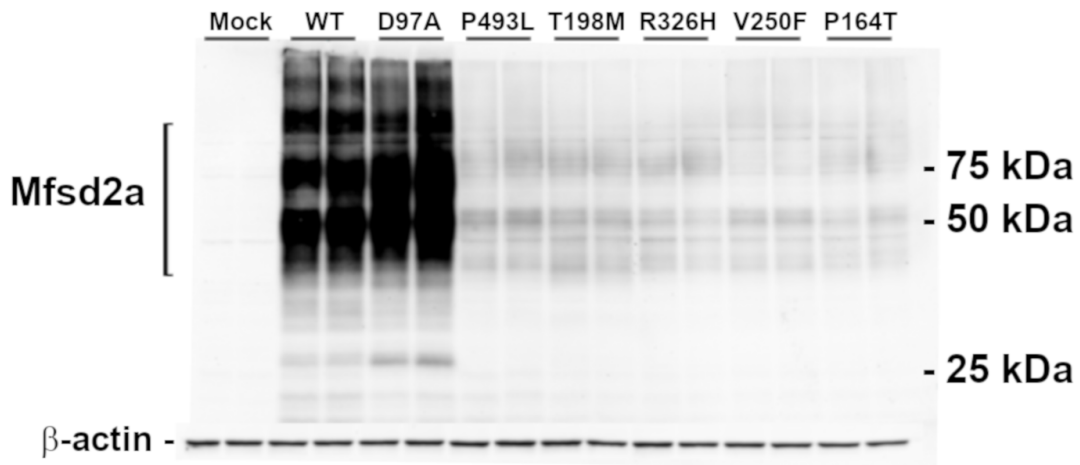
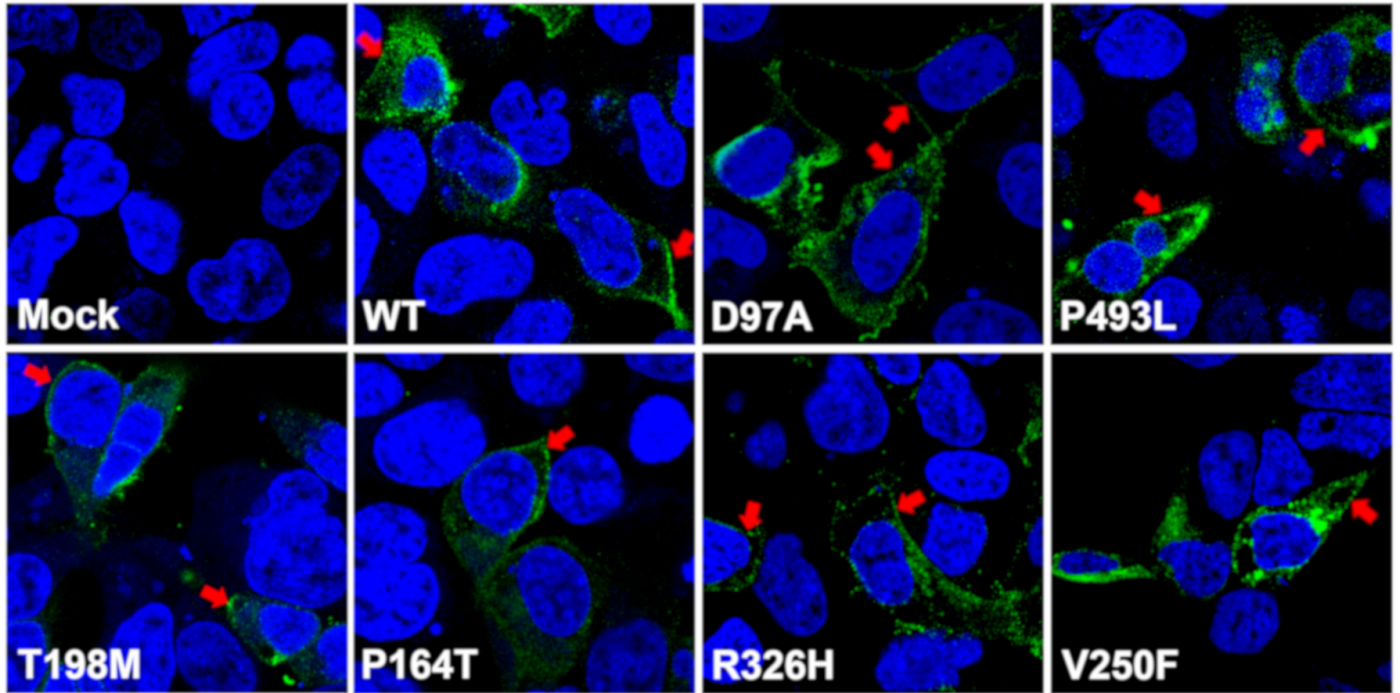
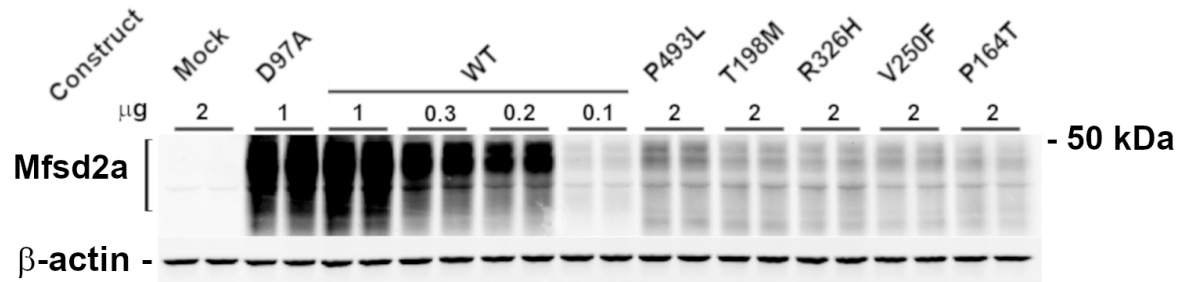
ASD Autism spectrum disorder Comp Het Compound heterozygous, DDH Developmental dysplasia of the hip F female, Fam Family, Hom Homozygous, FU Follow-up, M male, mo months, Mod moderate, N/A Not Applicable, OFC Occipito-frontal circumference, Pt Patient, TEV Talipes Equinovarus, y years. ‡ NG_053084.1(NM_032793.5): c.556+1G>A, NC_000001.11(NM_032793.5): c.556+1G>A, LRG_199t1). † Data available for 3 out of 4 patients. # PMID: 27457812. ## PMID: 30214071. ### PMID: 31585110.

Table 2. Frequency, conservation, and predicted functional impact of *MFSD2A* variants.

<i>MFSD2A</i> variant [NM_032793.5]	g. (hg19)	LOVD (ID)	Internal database ‡	ExAC/ gnomAD	GME	Iranome	Ensembl	ClinVar	SIFT	Mutation Taster	HSF/ VEP	GERP score	CADD score	ACMG class
c.476C>T (p.Thr159Met)	chr1:40431005 C>T	002760 75	-	0.000003 978 (1 het)	-	-	rs1057517 688	Pathogenic	Damaging (score 0)	Disease causing	-	5.75	34	Likely pathogenic (PS3, PM2, PP3, PP4, PP5)
c.593C>T (p.Thr198Met)	chr1:40431565 C>T	002760 71	-	0.000003 977 (1 het)	-	-	rs7564670 73	-	Damaging (score 0.003)	Disease causing	-	5.94	28.2	Likely pathogenic (PS3, PM2, PP3, PP4)
c.556+1G>A	chr1:40431222 G>A	002760 70	-	0.000003 978 (1 het)	-	-	rs7589530 00	-	-	Disease causing	WT donor site alteration	5.56	29.2	Pathogenic (PVS1, PM2, PP3, PP4)
c.750_753del (p.Cys251SerfsTer3)	chr1:40432304 TTGTC>T	002760 77	-	0.000003 982 (1 het)	-	-	-	-	-	Disease causing	-	-	-	Pathogenic (PVS1, PM2, PP4)
c.748G>T (p.Val250Phe)	chr1:40432306 G>T	002760 74	-	-	-	-	-	-	Damaging (score 0)	Disease causing	-	5.79	33	Likely pathogenic (PS3, PM2, PP3, PP4)
c.977G>A (p.Arg326His)	chr1:40432807 G>A	002760 74	-	0.000007 956 (2 het)	-	-	rs7767413 31	-	Tolerated (0.37 score)	Disease causing	-	5.52	24.4	Likely pathogenic (PS3, PM2, PP3, PP4)
c.1386_1435del (p.Gln462HisfsTer17)	chr1:40434271GCAG CCGGAACGTGTCA AGTTTACACTGAA CATGCTCGTGACC ATGGCTCC>G	002760 76	-	-	-	-	-	-	-	Disease causing	-	-	-	Pathogenic (PVS1, PM2, PP4)
c.1478C>T (p.Pro493Leu)	chr1:40434366 C>T	002760 67	-	-	-	-	-	-	Damaging	Disease causing	-	5.49	32	Likely pathogenic (PS3, PM2, PP3, PP4)

ACMG American College of Medical Genetics and Genomics, CADD Combined Annotation Dependent Depletion, GERP Genomic Evolutionary Rate Profiling, GME Greater Middle East Variome Project, HSF Human Splice Finder, LOVD-ID Leiden Open Variation Database Identifier, PVS pathogenic very strong, PS pathogenic strong, PM pathogenic moderate, PP pathogenic supporting, SIFT Sorting Intolerant From Tolerant, VEP Variant Effect Predictor, VUS variant of unknown significance.



a**b****c****d**